arXiv:1607.07513v1 [cond-mat.quant-gas] 26 Jul 2016

Quantum Defect Theory for Orbital Feshbach Resonance

Yanting Cheng,[1] Ren Zhang,[1,*] and Peng Zhang[2,3,4,†]

[1] *Institute for Advanced Study, Tsinghua University, Beijing, 100084, China*
[2] *Department of Physics, Renmin University of China, Beijing, 100872, China*
[3] *Beijing Computational Science Research Center, Beijing, 100084, China*
[4] *Beijing Key Laboratory of Opto-electronic Functional Materials & Micro-nano Devices (Renmin University of China)*

In the ultracold gases of alkali-earth (like) atoms, a new type of Feshbach resonance, i.e., the orbital Feshbach resonance (OFR), has been proposed and experimentally observed in ultracold ^{173}Yb atoms. When the OFR of the ^{173}Yb atoms occurs, the energy gap between the open and closed channels is smaller by two orders of magnitudes than the van der Waals energy. As a result, quantitative accurate results for the low-energy two-body problems can be obtained via multi-channel quantum defect theory (MQDT), which is based on the exact solution of the Schrödinger equation with the van der Waals potential. In this paper we use the MQDT to calculate the two-atom scattering length, effective range, and the binding energy of two-body bound states for the systems with OFR. With these results we further study the clock-transition spectrum for the two-body bound states, which can be used to experimentally measure the binding energy. Our results are helpful for the quantitative theoretical and experimental researches for the ultracold gases of alkali-earth (like) atoms with OFR.

PACS numbers: 03.65.-w,31.15.ac, 34.50.-s,34.50.Cx

I. INTRODUCTION

Feshbach resonance [1] is a powerful tool for the control of interaction between ultracold atoms [2]. In ultracold gases of alkali atoms the magnetic Feshbach resonances are widely used for the tuning of s-wave scattering lengths [2]. For the gases of ultracold alkali-earth (like) atoms, recently we found a new type of Feshbach resonance, i.e., the orbital Feshbach resonance (OFR) [3]. With the help of OFR, one can precisely control the s-wave scattering length between two fermionic alkali-earth (like) atoms in $^1S_0$ and $^3P_0$ electronic orbital states with different nuclear spin, by changing the magnetic field [3]. OFR has been experimentally observed in the ultracold gases of ^{173}Yb atoms [4, 5]. It is also shown that using the ultracold gases of alkali-earth (like) atoms with OFR one can study several interesting problems, including the Kondo effect, the strong-interacting ultracold fermi gases with narrow Feshbach resonance and the Leggett mode, *et. al.* [3, 6–14].

When the OFR of ^{173}Yb atoms occurs, the energy gap between the open and the closed channel is about 10^5Hz. It is by two orders of magnitude smaller than the characteristic energy of the inter-atom interaction (i.e., the van der Waals energy), which is of the order of 10^7Hz [4, 5, 15, 16]. As a result, a simple zero-range two-channel Huang-Yang pseudopotential can be used as an approximation for the inter-atom interaction [3, 16]. In this model, the two-body interaction is described by two parameters, i.e., the scattering lengths $a_\pm$ for the two independent scattering channels $|\pm\rangle$ which will be defined below. It is estimated that for ^{173}Yb atoms the quantitative precision of the OFR point given by the two-channel Huang-Yang pseudopotential is about 80% [3, 16].

To obtain more accurate results, one needs to take into account the effects from the finite range van der Waals interaction potential. To this end, one can numerically solve the multi-channel Schrödinger equation with a model interaction potential which behaves as a van der Waals potential in the long-range limit (*e.g.,* the Lenard-Jones potential) [12]. Nevertheless, there is also an analytical approach for the multi-channel low-energy two-body problem with van der Waals potential, i.e., the multi-channel quantum defect theory (MQDT) [18, 21–23] which is based on the analytical solution of the single-channel Schrödinger equation with van der Waals potential [17]. In ultracold atomic gas physics, this MQDT approach was originally developed for alkali atoms. Previous research for these systems shows that when the inter-channel energy gap is much smaller than the van der Waals energy, the result given by the MQDT is quantitatively very accurate [21, 23]. Thus, this approach is also applicable for the ultracold alkali earth (like) atoms with an OFR with small energy gaps between the open and the closed channels, *e.g.*, the ultracold ^{173}Yb atoms.

In this paper, using the MQDT we solve the low-energy two-body problems for alkali earth (like) atoms with an OFR. We derive the analytical expressions of the two-atom scattering length and effective range (Eqs. (42) and (43)), as well as the algebraic equation satisfied by the binding energy of two-body bound state (Eq. (52)). All the results are expressed in terms of the scattering length $a_\pm$ as well as the characteristic length β_6 of the van der Waals potential. Our results show that the OFR for ^{173}Yb atoms is a narrow resonance[7]. Using these results we further investigate the clock-transition spectrum of these systems, which can be used for the experimen-

*Electronic address: rine.zhang@gmail.com
†Electronic address: pengzhang@ruc.edu.cn

tal measurement of the binding energy. Our results are helpful for both theoretical and experimetnal study for ultracold alkali-earth (like) atoms with OFR.

The remainder of this manuscript is organized as follows. In Sec. II we show the MQDT approach for our system and calculate the two-atom s-wave scattering length and effective range. In Sec. III we calculate the binding energy and wave function of the two-atom bound state, as well as the clock-transition spectrum. Some summaries and discussions for our results are presneted in Sec. IV, and some details of our calculations are shown in the appendixes.

II. SCATTERING LENGTH AND EFFECTIVE RANGE

We consider two fermionic alkali-earth (like) atoms in $^1S_0$ (g) and $^3P_0$ (e) electronic orbital states, with nuclear-spin magnetic quantum numbers m_I ($\uparrow$) and $m_I + \Delta_m$ ($\downarrow$) (Fig. 1). The two-body internal state with one atom being in $|g,\downarrow\rangle$ and the other being in $|e,\uparrow\rangle$ can be denoted as

$$|o\rangle \equiv |g,\downarrow;e,\uparrow\rangle. \tag{1}$$

Similarly, we also denote the state with one atom being in $|g,\uparrow\rangle$ and the other being in $|e,\downarrow\rangle$ as

$$|c\rangle \equiv |g,\uparrow;e,\downarrow\rangle. \tag{2}$$

The Hamiltonian for the two-atom relative motion is given by

$$\hat{H} = -\frac{\hbar^2}{m}\nabla_{\mathbf{r}}^2 + \delta|c\rangle\langle c| + U(r), \tag{3}$$

where m is the single-atom mass, $\mathbf{r}$ is the relative position of these two atoms and $\delta = (\delta\mu)B$ is the Zeeman-energy difference between states $|c\rangle$ and $|o\rangle$, with $\delta\mu$ and B being the magnetic moment difference of these two states and the magnetic field, respectively. Without loss of generality, here we assume that $\delta\mu > 0$. In Eq. (3) $U(r)$ is the inter-atom interaction potential. It is diagonal in the bases

$$|\pm\rangle = \frac{1}{\sqrt{2}}\left(|c\rangle \mp |o\rangle\right), \tag{4}$$

and can be expressed as

$$U(r) = U^{(+)}(r)|+\rangle\langle+| + U^{(-)}(r)|-\rangle\langle-|, \tag{5}$$

where $U^{(\pm)}(r)$ is the potential curve with respect to state $|\pm\rangle$. When the two atoms are far away enough from each other, $U^{(\pm)}(r)$ can be approximated as the same van der Waals potential, i.e, we have

$$U^{(+)}(r > b) \approx U^{(-)}(r > b) \approx -\frac{\hbar^2\beta_6^4}{mr^6}. \tag{6}$$

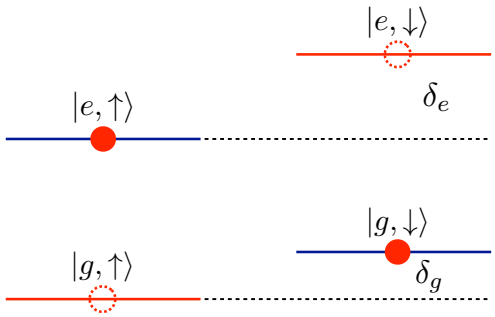

FIG. 1: (color online) Energy level diagram of a single atom. For the OFR, the open channel $|o\rangle$ is the two-body internal state with one atom being in $|g,\downarrow\rangle$ and the other being in $|e,\uparrow\rangle$ (the red filled circles), while the closed channel $|c\rangle$ is the state where one atom being in $|g,\uparrow\rangle$ and the other being in $|e,\downarrow\rangle$ (the red unfilled circles with dashed line). Here $\delta_e = \mu_e\Delta_m B$ is the Zeeman-energy difference between the single-atom states $|e,\downarrow\rangle$ and $|e,\uparrow\rangle$, and $\delta_g = \mu_g\Delta_m B$ is the one between states $|g,\downarrow\rangle$ and and $|g,\uparrow\rangle$, with $\mu_{e(g)}$ being the magnetic moment for the electronic orbital state $|e\rangle$ ($|g\rangle$). The Zeeman energy difference δ in Eq. (3) can be expressed as $\delta = \delta_e - \delta_g = (\delta\mu)B$ with $\delta\mu = (\mu_e - \mu_g)\Delta_m$.

Here β_6 is the characteristic length of the van der Waals potential and the range b satisfies the conditions

$$b < \beta_6; \tag{7}$$

$$\frac{\hbar^2\beta_6^4}{mb^6} \gg \frac{\hbar^2}{m\beta_6^2}. \tag{8}$$

In this paper we focus on the systems where the energy gap δ between the states $|c\rangle$ and $|o\rangle$ is much smaller than the van der Waals energy $\hbar^2/(m\beta_6^2)$. As shown below, our finial result is independent of the exact value of b.

We consider the s-wave scattering of two atoms incident from channel $|o\rangle$, with relative momentum $\hbar k$. Here we assume the scattering energy

$$\epsilon = \frac{\hbar^2k^2}{m} \tag{9}$$

is smaller than the inter-channel energy gap δ. As a result, in the scattering process the channel $|o\rangle$ is open while the channel $|c\rangle$ is closed.

The s-wave scattering length and effective range is determined by the two-atom scattering wave function $|\psi_{\epsilon,\delta}(r)\rangle$ which satisfies the Schrödinger equaiton

$$\hat{H}|\psi_{\epsilon,\delta}(r)\rangle = E|\psi_{\epsilon,\delta}(r)\rangle \tag{10}$$

with the boundary conditions

$$\lim_{r\to 0}\left[r\langle r|\psi_{\epsilon,\delta}(r)\rangle\right] = 0 \tag{11}$$

and

$$\lim_{r\to\infty}\langle c|\psi_{\epsilon,\delta}(r)\rangle \to 0. \tag{12}$$

It is pointed out that, if we solve Eq. (10) only with the the boundary condition (11), we can get *two* linearly-independent special solutions. The solution of Eq. (10) and conditions (11, 12), i.e., the scattering wave function $|\psi_{\epsilon,\delta}(r)\rangle$, can be expressed as the superposition of these two special solutions. Following the idea of MQDT, below we will first derive the special solutions of Eq. (10) and the condition (11) for the simple case with $\delta = 0$, and then derive the special solutions of (10) and (11) for non-zero δ. Finally, we will construct the scattering wave function $|\psi_{\epsilon,\delta}(r)\rangle$ with these special solutions and the condition (12). With this wave function we can derive the s-wave scattering phase shift, scattering length and effective range.

A. Special Solutions of Eqs. (10) and (11) for $\delta = 0$

When $\delta = 0$, the Hamiltonian $\hat{H}$ given by Eq. (3) is diagonal in the bases $\{|+\rangle, |-\rangle\}$. Therefore, in this case we can choose the two special solutions of Eq. (10) and (11) as

$$|\psi^{(+)}_{\epsilon,\delta=0}(r)\rangle = \frac{\phi^{(+)}_{\epsilon}(r)}{r}|+\rangle; \tag{13}$$

$$|\psi^{(-)}_{\epsilon,\delta=0}(r)\rangle = \frac{\phi^{(-)}_{\epsilon}(r)}{r}|-\rangle. \tag{14}$$

Substituting Eqs. (13, 14) into Eq. (10), we obtain two equaitons for the components $\phi^{(\pm)}_{\epsilon}(r)$:

$$-\frac{\hbar^2}{m}\frac{d^2}{dr^2}\phi^{(\pm)}_{\epsilon}(r) + U^{(\pm)}(r)\phi^{(\pm)}_{\epsilon}(r) = \epsilon\phi^{(\pm)}_{\epsilon}(r). \tag{15}$$

Furthermore, using the epression (6) of the potential $U^{(\pm)}(r)$ in the region $r > b$, in this region we can reduce these two equations to

$$-\frac{d^2}{dr^2}\phi^{(\pm)}_{\epsilon}(r) - \frac{\beta_6^4}{r^6}\phi^{(\pm)}_{\epsilon}(r) = k^2\phi^{(\pm)}_{\epsilon}(r). \tag{16}$$

Thus, when $r > b$ the components $\phi^{(\pm)}_{\epsilon}(r)$ can be expressed as the superpositions of two special solutions $f^0_{\epsilon}(r)$ and $g^0_{\epsilon}(r)$ of Eq. (16), which were analytically derived by Bo Gao in Ref. [17]. Namely, we can choose $\phi^{(\pm)}_{\epsilon}(r)$ to satisfy

$$\phi^{(\pm)}_{\epsilon}(r > b) = f^0_{\epsilon}(r) - K^0_{\pm}g^0_{\epsilon}(r), \tag{17}$$

where the parameters $K^0_{\pm}$ are determined by the short-range detail of the potential curves $U^{(\pm)}(r)$ in the region $r < b$. In this paper we consider the case where the scattering energy ϵ is much smaller than the van der Waals energy $\hbar^2/(m\beta_6^2)$. Due to the conditions (7) and (8), ϵ is also much smaller than $\hbar^2/(mb^2)$. In this case the behavior of $\phi^{(\pm)}_{\epsilon}(r)$ in the region around $r = b$ is almost independent of ϵ. Furthermore, it is also shown that the functions $f^0_{\epsilon}(r)$ and $g^0_{\epsilon}(r)$ are almost ϵ-independent when $r \approx b$ [17]. Thus, the parameters $K_{\pm}$ is alsom almost independent of ϵ. That is one of the basic ideas of the QDT [18–20].

For $\epsilon > 0$, in the limit $r \to \infty$ we have [17]

$$\lim_{r\to\infty} f^0_{\epsilon}(r) = \sqrt{\frac{2}{\pi k}}\left[Z_{ff}(\epsilon)\sin(kr) - Z_{fg}(\epsilon)\cos(kr)\right]; \tag{18}$$

$$\lim_{r\to\infty} g^0_{\epsilon}(r) = \sqrt{\frac{2}{\pi k}}\left[Z_{gf}(\epsilon)\sin(kr) - Z_{gg}(\epsilon)\cos(kr)\right], \tag{19}$$

where

$$k = \frac{\hbar}{\sqrt{m\epsilon}}, \tag{20}$$

and the functions $Z_{ij}(\epsilon)$ $(i, j = f, g)$ are given in Ref. [17]. Substituting Eq. (18, 19) into Eqs. (17) and using the expressions of s $Z_{ij}(\epsilon)$, one can obtain [18]

$$\lim_{r\to\infty} \phi^{(\pm)}_{\epsilon=0}(r) \propto \left[r - \frac{(2\pi)(K^0_{\pm} - 1)}{\Gamma(1/4)^2 K^0_{\pm}}\beta_6\right]. \tag{21}$$

On the other hand, since in our case with $\delta = 0$ the states $|+\rangle$ and $|-\rangle$ are two independent scattering channels, we also have $\lim_{r\to\infty} \phi^{(\pm)}_{\epsilon=0}(r) \propto (r - a_s^{(\pm)})$ where $a_s^{(\pm)}$ is the s-wave scattering length for each channel. Thus, Eq. (21) implies the relation between parameter $K^0_{\pm}$ and the scattering length $a_s^{(\pm)}$ [18]:

$$K^0_{\pm} = \frac{2\pi\beta_6}{2\pi\beta_6 - a_s^{(\pm)}\Gamma(1/4)^2}. \tag{22}$$

B. Special Solutions of Eqs. (10) and (11) for $\delta \neq 0$

Now we consider the special solutions of Eq. (10) and condition (11) for the case with $\delta \neq 0$. As mentioned above, in this subsection we ignore the boundary condition (12). When $\delta \neq 0$, it is convenient to expand $|\psi_{\epsilon,\delta}(r)\rangle$ in the bases $\{|c\rangle, |o\rangle\}$. Since the potential $U^{(\pm)}(r)$ satisfies the condition (6), in the region $r > b$ the interaction U is independent on the internal state of these two atoms. As a result, the channels $|c\rangle$ and $|o\rangle$ are decoupled and Eq. (10) can be simplified as

$$\left[-\frac{d^2}{dr^2} - \frac{\beta_6^4}{r^6}\right][r\langle o|\psi_{\epsilon,\delta}(r)\rangle] = \epsilon\,[r\langle o|\psi_{\epsilon,\delta}(r)\rangle]; \tag{23}$$

$$\left[-\frac{d^2}{dr^2} - \frac{\beta_6^4}{r^6}\right][r\langle c|\psi_{\epsilon,\delta}(r)\rangle] = (\epsilon - \delta)\,[r\langle c|\psi_{\epsilon,\delta}(r)\rangle]. \tag{24}$$

Therefore, similar as in Sec. II. A, for $r > b$ the component $r\langle o|\psi_{\epsilon,\delta}(r)\rangle$ can be expressed as the superpositions of functions $f^0_{\epsilon}(r)$ and $g^0_{\epsilon}(r)$, and $r\langle c|\psi_{\epsilon,\delta}(r)\rangle$can be

expressed as the superpositions of $f^0_{\epsilon-\delta}(r)$ and $g^0_{\epsilon-\delta}(r)$. Thus, we can choose the two special solutions of $|\psi^{(\alpha,\beta)}_{\epsilon,\delta}(r)\rangle$ of Eq. (10) to satisfy

$$\begin{aligned} &|\psi^{(\alpha)}_{\epsilon,\delta}(r>b)\rangle \\ &= \frac{1}{r}\{\left[f^0_\epsilon(r) - K^0_{oo}g^0_\epsilon(r)\right]|o\rangle - K^0_{co}g^0_{\epsilon-\delta}(r)|c\rangle\}, \quad (25) \\ &|\psi^{(\beta)}_{\epsilon,\delta}(r>b)\rangle \\ &= \frac{1}{r}\{-K^0_{oc}g^0_\epsilon(r)|o\rangle + \left[f^0_{\epsilon-\delta}(r) - K^0_{cc}g^0_{\epsilon-\delta}(r)\right]|c\rangle\}. \end{aligned} \quad (26)$$

Here the parameter K^0_{ij} $(i,j=o,c)$ is also determined by the detail of the potential curves $U^{(\pm)}(r)$ in the region $r<b$. Similar as in Sec. II. A, due to the conditions (7, 8) and the fact that both ϵ and δ are much smaller than $\hbar^2/(m\beta_6^2)$, the values of K^0_{ij} $(i,j=o,c)$ is independent of both the scattering energy ϵ and the energy gap δ [21] (Appendix A). Therefore, we can obtain the values of K^0_{ij} $(i,j=o,c)$ from the behaivor of $|\psi^{(\alpha,\beta)}_{\epsilon,\delta}(r)\rangle$ in the limit $\delta\to 0$ with the following analysis: in Sec. II. A we have already obtained two special solutions $|\psi^{(\pm)}_{\epsilon,\delta=0}(r)\rangle$ for Eqs. (10) and (11) with $\delta=0$. Therefore, $|\psi^{(\alpha,\beta)}_{\epsilon,\delta=0}(r)\rangle$ should be the linear combinations of these two solutions, i.e., $|\psi^{(\alpha,\beta)}_{\epsilon,\delta}(r)\rangle$ can be expressed as

$$|\psi^{(\alpha)}_{\epsilon,\delta=0}(r>b)\rangle = A_1|\psi^{(+)}_{\epsilon,\delta=0}(r>b)\rangle + A_2|\psi^{(-)}_{\epsilon,\delta=0}(r>b)\rangle; \quad (27)$$

$$|\psi^{(\beta)}_{\epsilon,\delta=0}(r>b)\rangle = A_3|\psi^{(+)}_{\epsilon,\delta=0}(r>b)\rangle + A_4|\psi^{(-)}_{\epsilon,\delta=0}(r>b)\rangle, \quad (28)$$

with $A_{1,2,3,4}$ being r-independent coefficient. Substituting Eqs. (25, 26) into the left-hand side of Eqs. (27, 28), and substituting Eqs. (13, 14, 17) into the ringt-hand side of Eqs. (27, 28) we find that

$$K^0_{cc} = K^0_{oo} = \frac{1}{2}\left(K^0_+ + K^0_-\right); \quad (29)$$

$$K^0_{co} = K^0_{oc} = \frac{1}{2}\left(K^0_- - K^0_+\right). \quad (30)$$

Moreover, with the relation (22) the parameters K^0_{ij} $(i,j=o,c)$ can be further expressed as functions of β_6 and the scattering length $a_s^{(\pm)}$.

C. Scattering Wave Function and Phase Shift

Now we calculate the scattering wave function $|\psi_{\epsilon,\delta}(r)\rangle$ which satisfies Eq. (10) and both of the two boundary conditions (11) and (12). This scattering state is the superposition of the two special solutions $|\psi^{(\alpha,\beta)}_{\epsilon,\delta}(r)\rangle$ of Eqs. (10) and (11), which were derived in Sec. II. B. Namely, $|\psi_{\epsilon,\delta}(r)\rangle$ can be expressed as

$$|\psi_{\epsilon,\delta}(r)\rangle = B\left\{|\psi^{(\alpha)}_{\epsilon,\delta}(r)\rangle + C|\psi^{(\beta)}_{\epsilon,\delta}(r)\rangle\right\}, \quad (31)$$

where the coefficient C is determined by the condition (12) and the coefficient B could be arbitrary r-independent constant. In addition, according to this result and Eqs. (25, 26), in the region $r>b$ the component $\langle c|\psi_{\epsilon,\delta}(r)\rangle$ is a linear combination of functions $f^0_{\epsilon-\delta}(r)$ and $g^0_{\epsilon-\delta}(r)$. In our system with $\epsilon<\delta$, these two functions satisfy [18]

$$\lim_{r\to\infty} f^0_{\epsilon-\delta}(r) = \frac{1}{\sqrt{2\pi\kappa}}\left[W_{f-}(\epsilon-\delta)e^{\kappa r} + W_{f+}(\epsilon-\delta)e^{-\kappa r}\right]; \quad (32)$$

$$\lim_{r\to\infty} g^0_{\epsilon-\delta}(r) = \frac{1}{\sqrt{2\pi\kappa}}\left[W_{g-}(\epsilon-\delta)e^{\kappa r} + W_{g+}(\epsilon-\delta)e^{-\kappa r}\right], \quad (33)$$

where

$$\kappa = \frac{\sqrt{m(\delta-\epsilon)}}{\hbar} \quad (34)$$

and the funcitons $W_{ij}(z)$ $(i=f,g;\ j=\pm)$ are discussed in Ref. [18]. Substituting Eqs. (32, 33) into Eq. (31), we can express $\lim_{r\to\infty}\langle c|\psi_{\epsilon,\delta}(r)\rangle$ in terms of parameter C. Moreover, matching this expression with the boundary condition (12), we found that

$$C = \frac{K_{co}W_{g-}(\epsilon-\delta)}{W_{f-}(\epsilon-\delta) - K_{cc}W_{g-}(\epsilon-\delta)}. \quad (35)$$

Substituting this expression into Eq. (31), we obtain the component of the scattering wave function $|\psi_{\epsilon,\delta}(r)\rangle$ in the open channel:

$$\langle o|\psi_{\epsilon,\delta}(r>b)\rangle = \frac{B}{r}\left\{f^0_\epsilon(r) - K_{\rm eff}\left[\epsilon,\delta\right]g^0_\epsilon(r)\right\}, \quad (36)$$

where the function $K_{\rm eff}[\epsilon,\delta]$ is defined as

$$K_{\rm eff}\left[\epsilon,\delta\right] = K^0_{oo} + \frac{K^0_{oc}K^0_{co}}{\chi(\epsilon-\delta) - K^0_{cc}}. \quad (37)$$

Here K^0_{ij} $(i,j=o,c)$ are given in Eqs. (29, 30), with $K^0_\pm$ being given in Eq. (22), and the function $\chi(z)$ is defined as

$$\chi(z) = \frac{W_{f-}(z)}{W_{g-}(z)}. \quad (38)$$

Substituting Eqs. (18, 19) into Eq. (36), we can further obtain the behavior of $\langle o|\psi_{\epsilon,\delta}(r)\rangle$ in the limit $r\to\infty$. Comparing this expression with the relation

$$\lim_{r\to 0}\langle o|\psi_{\epsilon,\delta}(r)\rangle \propto \frac{1}{r}\left[\cot\eta_0(k)\sin(kr) + \cos(kr)\right], \quad (39)$$

where η_0 is the s-wave scattering phase shift, we finally find that $\tan\eta_0(k)$ can be expressed as

$$\cot\eta_0(k) = \frac{Z_{ff}(\epsilon) - K_{\rm eff}\left[\epsilon,\delta\right]Z_{gf}(\epsilon)}{K_{\rm eff}\left[\epsilon,\delta\right]Z_{gg}(\epsilon) - Z_{fg}(\epsilon)}. \quad (40)$$

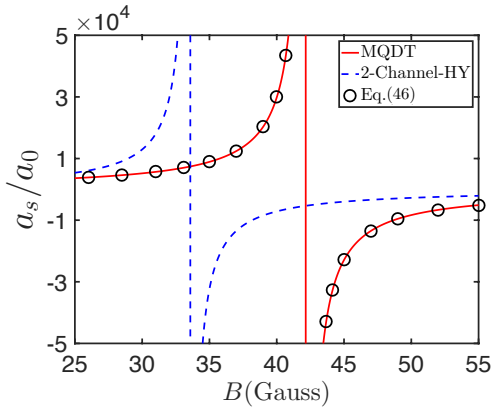

FIG. 2: (color online) The s-wave scattering length a_s of ^{173}Yb atoms, as a function of magnetic field. Here we show the results given by the MQDT (i.e., Eq. (42)) (red solid line), the 2-channel Huang-Yang (HY) pesudopotential (i.e., Eq. (45)) (blue dashed line) and the result from the approximated expression (46) (black circles). We consider the case with $\Delta_m = 5$ and take $a_s^{(+)} = 1900a_0$, $a_s^{(-)} = 200a_0$, $\beta_6 = 169.6a_0$ with a_0 being the Bohr's radius, and $\mu_e - \mu_g = 2\pi\hbar \times 112$Hz/Gauss.

Moreover, since $K_{\rm eff}[\epsilon, \delta]$ is determined by the parameters $K_{ij}^{(0)}$ $(i, j = o, c)$ and $K_{ij}^{(0)}$ is a function of the scattering lengths $a_s^{(\pm)}$ and the characteristic length β_6 of the van der Waals interaction potential, $\tan\eta_0(k)$ given by Eq. (40) is essentially a function of $a_s^{(\pm)}$, β_6, δ and ϵ. Here we point out that, the expression (40) of $\tan\eta_0(k)$ has the same form as the one for the case with a single-channel van der Waals potential (i.e., Eq.(5) of Ref.[18]), while the parameter K_0 for the single-channel case should be replaced by $K_{\rm eff}[\epsilon, \delta]$ for our case.

D. s-wave Scattering Length and Effective Range

Using Eq. (40) we can calculate the two-atom s-wave scattering length a_s and effective range $r_{\rm eff}$ which are defined via the low-energy expansion of $k\cot\eta_0(k)$:

$$k\cot\eta_0(k) = -\frac{1}{a_s} + \frac{1}{2}r_{\rm eff}k^2 + \mathcal{O}(k^3). \tag{41}$$

Substituting Eq. (40) into Eq. (41) and using direct calculations which are quite similar to the single-channel case [18], we can obtain

$$a_s(\delta) = \frac{2\pi}{[\Gamma(1/4)]^2}\frac{K_{\rm eff}[0,\delta]-1}{K_{\rm eff}[0,\delta]}\beta_6, \tag{42}$$

$$r_{\rm eff}(\delta) = \frac{[\Gamma(1/4)]^2}{3\pi}\frac{K_{\rm eff}[0,\delta]^2+1}{(K_{\rm eff}[0,\delta]-1)^2}\beta_6 + \frac{[\Gamma(1/4)]^2}{\pi}\frac{\hbar^2 K'_{\rm eff}[0,\delta]}{m\beta_6\,(K_{\rm eff}[0,\delta]-1)^2}, \tag{43}$$

where $K'_{\rm eff}[\epsilon,\delta] = dK'_{\rm eff}[\epsilon,\delta]/d\epsilon$. In addition, with the help of the relation $\delta = (\delta\mu)B$ we can further express a_s and $r_{\rm eff}$ as functions of the magnetic field B. It is clear that we have $a_s = \infty$ at the magnetic field B_0 which satisfies the condition

$$K_{\rm eff}[0, (\delta\mu B_0)] = 0. \tag{44}$$

That is the OFR.

In Fig. 2, we illustrate the scattering length a_s for ^{173}Yb with $a_s^{(+)} = 1900a_0, a_s^{(-)} = 200a_0$[5] and $\beta_6 = 169.6a_0$[15], with a_0 being the Bohr's radius. Here we consider the case with $\Delta_m = 5$. For comparison, we also show a_s given by the zero-range two-channel Huang-Yang pseudopotential, which can be expressed as [3, 16],

$$a_s = \frac{-[a_s^{(+)}+a_s^{(-)}] + 2\sqrt{m\delta/\hbar^2}a_s^{(+)}a_s^{(-)}}{[a_s^{(+)}+a_s^{(-)}]\sqrt{m\delta/\hbar^2}-1}. \tag{45}$$

As show in Fig. 2, the difference between the OFR points given by the MQDT and the 2-channel Huang-Yang pseudopotential is about 9G, and the relative difference is about 20%.

On the other hand, around the OFR point B_0 the scattering length a_s can be expanded as a series of $1/(B-B_0)$. By neglecting the high-order terms, we obtain the approximate expression of a_s :

$$a_s \approx a_{\rm bg}\left(1 - \frac{\Delta_B}{B-B_0}\right). \tag{46}$$

Our calculation show that for ^{173}Yb we have $a_{\rm bg} = -98a_0$ and $\Delta_B = -660G$. As shown in Fig. 2, this approximate expression is quantitatively consistent with the MQDT result (i.e., Eq.(42)) in a large range of magnetic field.

In Fig. 3 we illustrate the effective range $r_{\rm eff}$ for the OFR of ^{173}Yb atoms with $\Delta_m = 5$. Our calculation shows that at the OFR point we have $|r_{\rm eff}| \approx 908.7a_0 \approx 5.4\beta_6$ and thus the resonance parameter $s_{\rm res} \equiv 4\pi\beta_6/(\Gamma(1/4)^2 r_{\rm eff})$ is about 0.18. This means that OFR for ^{173}Yb is a narrow resonance in the sense of effective range[2, 7].

It is pointed that the effective range diverges in the limit $B \to 0$, as shown in Fig. 3. That is due to the fact that the function $\frac{d\chi(z)}{dz}|_{z=-\delta}$, which is proportional to $K'[0,\delta]$, diverges in the limit $\delta \to 0$. This result may also be understood with the following analysis. We consider the scattering of two atoms incident from the open channel $|o\rangle$. When the scattering energy ϵ is smaller than the energy gap δ between the open and closed channels, there is only elastic scattering between these two atoms. Accordingly, the parameter $k\cot\eta_0$ defined by Eq. (39) is real. Nevertheless, when $\epsilon > \delta$ there are both elastic scattering in channel $|o\rangle$ and the inelastic scattering from channel $|o\rangle$ to $|c\rangle$. As a result, the imaginary part of $k\cot\eta_0$ becomes nonzero. Therefore, as a function of k, the factor $k\cot\eta_0$ is not analytical at the point $k = \sqrt{\delta}$. Thus, the convergence radius of the low-energy expansion (41) is at most $\sqrt{\delta}$. Therefore, in the limit $B \to 0$ which yields $\delta \to 0$, the convergence radius of (41) tends to zero. As a result, the expansion coefficient $r_{\rm eff}$ diverges.

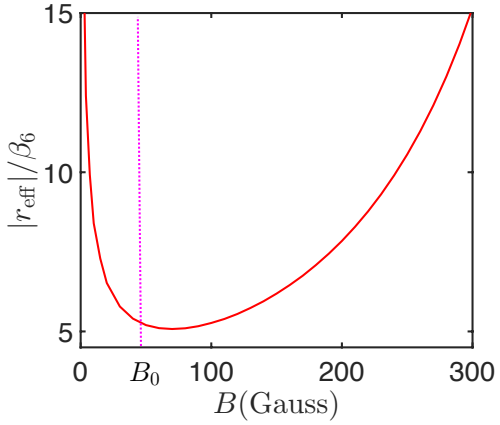

FIG. 3: (color online) The effective range $r_{\rm eff}$ of ^{173}Yb atoms given by the MQDT. Here the pink dotted line indicates the OFR point B_0. In our calculation we use the same parameter as in Fig. 2.

III. TWO-ATOM BOUND STATE

In this section we investigate the two-atom bound state in the system with OFR. We will calculate the binding energy and wave function with MQDT and study the clock-transition spectrum for the bound state, which may be observed in the experiments.

A. Binding Energy and Wave Function

In our system the two-body bound state wave function $|\phi_b(r)\rangle$ and the bound-state energy E_b satisfy the Schrödinger equation

$$\hat{H}|\phi_b(r)\rangle = E_b|\phi_b(r)\rangle \tag{47}$$

as well as the conditions

$$\lim_{r\to 0}(r|\phi_b(r)\rangle) = 0; \tag{48}$$

$$\lim_{r\to\infty}|\phi_b(r)\rangle = 0, \tag{49}$$

and

$$E_b < 0. \tag{50}$$

Here we consider the cases where the binding energy $|E_b|$ is much smaller than $\hbar^2/(m\beta_6^2)$. In these cases we can derive E_b with the MQDT approach introduced above. With the analysis shown in the above section, we can obtain two special solutions $|\psi^{(\alpha)}_{E_b,\delta}(r)\rangle$ and $|\psi^{(\beta)}_{E_b,\delta}(r)\rangle$ for Eqs. (47) and (48). In the region $r > b$, the solutions $|\psi^{(\alpha,\beta)}_{E_b,\delta}(r)\rangle$ also satisfy Eqs. (25, 26) with K^0_{ij} $(i,j = o,c)$ being given by Eqs. (29, 30) and $\epsilon = E_b$. The bound-state wave function $|\phi_b(r)\rangle$ can be expressed as the superposition of these two special solutions, i.e., we have

$$|\phi_b(r)\rangle = C_\alpha|\psi^{(\alpha)}_{E_b,\delta}(r)\rangle + C_\beta|\psi^{(\beta)}_{E_b,\delta}(r)\rangle, \tag{51}$$

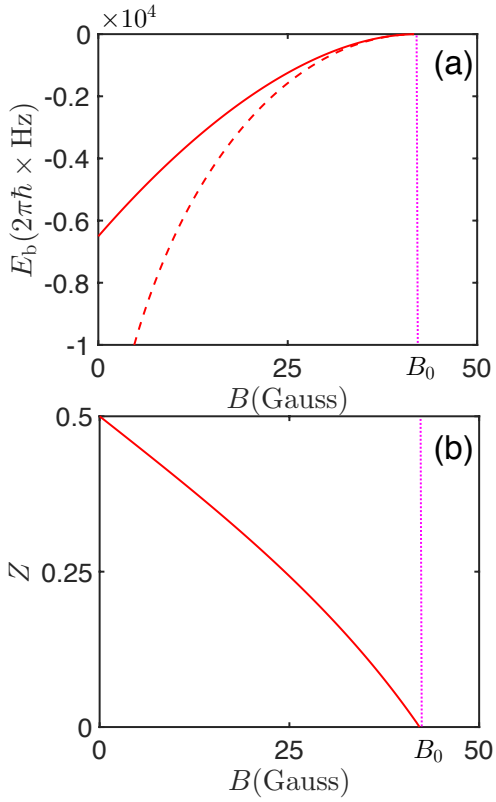

FIG. 4: (color online) The bound-state energy E_b (a) and closed-channel population Z (b) of ^{173}Yb atoms. Here we show the value of E_b given by the MQDT (red solid line) and the simple expression $E_s \equiv -\hbar^2/ma_s^2$ (red dashed line). In our calculation we use the same parameter as in Fig. 2. Here the pink dotted line indicates the OFR point B_0.

with $C_{\alpha,\beta}$ the superposition coefficients. Furthermore, substituting the behaviors of the functions $f^{(0)}_\epsilon(r)$ and $g^{(0)}_\epsilon(r)$ in the long-range limit $r\to\infty$, i.e., Eqs. (2) and (3) of Ref.[18], we can derive the long-range behavior of the special solutions $|\psi^{(\alpha,\beta)}_{E_b,\delta}(r)\rangle$. Substituting this behavior into the expression (51) and then into the boundary conditions (48, 49), we can finally derive the algebraic equation satisfied by the bound-state energy E_b

$$\chi(E_b) = K_{\rm eff}[E_b,\delta], \tag{52}$$

with the function $\chi(z)$ and $K_{\rm eff}[z,\delta]$ being introduced in Sec. II. C. We can obtain the energy E_b by solving Eq. (52).

Furthermore, we can also calculate the closed-channel population Z of the two-body bound state, which is defined as

$$Z \equiv \frac{\int |\langle c|\phi_b(r)\rangle|^2 d\mathbf{r}}{\int \left[|\langle c|\phi_b(r)\rangle|^2 + |\langle o|\phi_b(r)\rangle|^2\right] d\mathbf{r}}. \tag{53}$$

Using the Feynmann-Hellman theorem, it can be prove that the value of Z is given by the derivative of the bound-state energy E_b with respect to the energy gap

δ between the open and closed channels:

$$Z = \frac{\partial E_b}{\partial \delta}. \tag{54}$$

In Fig. 4 (a, b) we illustrate the bound-state energy E_b and the closed-channel population Z for ^{173}Yb atoms, as functions of the magnetic field B. For comparison, we also show the energy given by the the simple expression $E_s \equiv -\hbar^2/ma_s^2$ with a_s being the s-wave scattering length given by the MQDT. For a wide Feshbach resonance which is dominated by the open channel, we have $E_b \approx E_s$ and $Z \approx 0$ in a broad region around the resonance point. Nevertheless, as shown in Fig. 4 (a, b), in most of the resonance region of ^{173}Yb atoms the behaviors of E_b and E_s are quite different with each other and the closed-channel population Z is significantly non-zero. These results also imply that the OFR for ^{173}Yb is a narrow resonance in which the contribution from the closed channel is quite significant. That is consistent with our previous analysis based on the effective range.

B. Clock-Transition Spectrum

Now we investigate the clock-transition spectrum for the ultracold gases of alkali-earth (like) atoms in the two-body bound state $|\phi_b(r)\rangle$ (i.e., the ultracold gases of dimers). It is clear that in each dimer one atom is in the electronic orbital g-state and the other atom is in the e-state. Therefore, if a pulse of clock laser with π-polarization, which can induce the one-body transition (clock transition) between states $|g,j\rangle$ and $|e,j\rangle$ ($j =\uparrow,\downarrow$), is applied to these two atoms, the dimer may be dissociated into two free atoms via the following two first-order processes (Fig. 5):

(I) The atom in g-state absorbs a photon and transit to the e-state. After this process both of the two atoms are in the e-state. Since in $|\phi_b(r)\rangle$ one atom is in nuclear-spin state $\uparrow$ and other atom is in state $\downarrow$, and the π-laser beam does not change nuclear-spin state, after this process we have one atom in state $|e,\uparrow\rangle$ and the other atom in state $|e,\downarrow\rangle$. Furthermore, the center of mass (CoM) of these two atoms can obtain a recoil momentum $\hbar\mathbf{k}_\mathrm{L}$ from the laser photon, with $\mathbf{k}_\mathrm{L}$ being the wave vector of the clock laser.

(II) The atom in e-state emit a photon and transit to the g-state. With similar analysis, we know that after this process one atom is in state $|g,\uparrow\rangle$ and the other atom is in state $|g,\downarrow\rangle$, and the CoM can also obtain a recoil momentum $-\hbar\mathbf{k}_\mathrm{L}$.

Now we study the properties of the clock-transition spectrum, i.e., the dissociation rate as a function of the clock-laser angular frequency ω_L. We first consider the energy condition of the above two processes. Before the transition process, the energy of these two atoms is

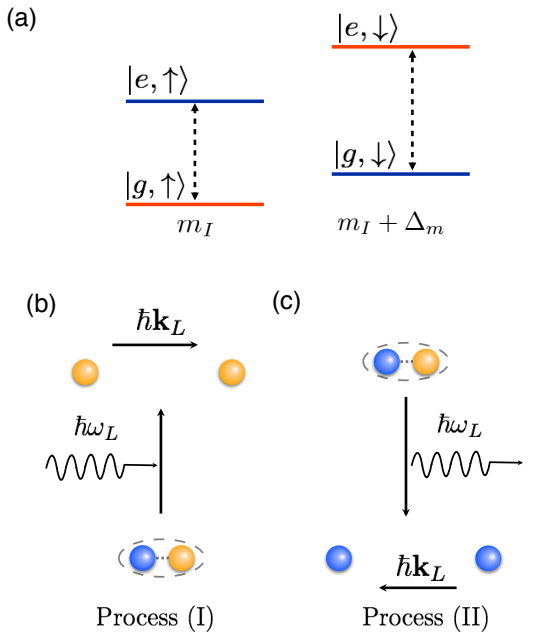

FIG. 5: (color online) (a): Schematic diagram for the experiment of clock-transition spectrum. The π-polarized clock laser can induce one-body transition between states $|g,\uparrow\rangle$ and $|e,\uparrow\rangle$, as well as the transition between $|g,\downarrow\rangle$ and $|e,\downarrow\rangle$. As defined in Sec. II, m_I and $m_I + \Delta_m$ are the magnetic quantum numbers for the nuclear spin states $\uparrow$ and $\downarrow$, respectively. (b) and (c): Two processes of clock-laser-induced dissociation of a dimer, where one atom (the yellow atom) is in the e-state and the other atom (the blue atom) is in the g-state. Process (I): the atom in the g-state absorbs a photon and transit to the e-state. The two-atom mass center gain a photon recoil momentum $\hbar\mathbf{k}_\mathrm{L}$. Process (II): the atom in e-state emit a photon and transit to the g-state. The two-atom mass center gain a photon recoil momentum $-\hbar\mathbf{k}_\mathrm{L}$.

$$E_0 = E_{e\uparrow} + E_{g\downarrow} - |E_b| + \frac{\hbar^2|\mathbf{K}|^2}{4m}, \tag{55}$$

where $\hbar\mathbf{K}$ is the CoM momentum. Here E_{lj} ($l = e,g$, $j =\uparrow,\downarrow$) is the energy of the one-atom internal state $|l,j\rangle$, and can be expressed as $E_{g\uparrow} = \mu_g m_I B$, $E_{g\downarrow} = \mu_g(m_I + \Delta_m)B$, $E_{e\uparrow} = \epsilon_{eg} + \mu_e m_I B$ and $E_{e\downarrow} = \epsilon_{eg} + \mu_e(m_I + \Delta_m)B$, with ϵ_{eg} being the energy gap between e-state and g-state for $B = 0$. The term $E_{e\uparrow} + E_{g\downarrow}$ in Eq. (55) is nothing but the threshold energy of the open channel $|o\rangle$. Now we consider the process (I) in which the atoms absorb a photon. Due to the energy-conservation, this process can occur under the condition

$$E_0 + \hbar\omega_\mathrm{L} > E^{(\mathrm{I})}_{\mathrm{min}}, \tag{56}$$

where $E^{(\mathrm{I})}_{\mathrm{min}}$ is the minimum energy of the finial states of process (I). Furthermore, since the finial state of process (I) is a scattering state of two atoms in state $|e,\uparrow\rangle$ and $|e,\downarrow\rangle$, with mass-center momentum $\hbar(\mathbf{K} + \mathbf{k}_\mathrm{L})$, the

minimum energy of the finial state of process (I) is

$$E_{\min}^{(\mathrm{I})} = E_{e\uparrow} + E_{e\downarrow} + \frac{\hbar^2|\mathbf{K}+\mathbf{k}_{\mathrm{L}}|^2}{4m}. \tag{57}$$

Thus, the energy condition (56) for process (I) can be re-written as

$$\omega_{\mathrm{L}} > \omega_{\mathrm{I}}(\mathbf{K}) \equiv \frac{E_{e\downarrow} - E_{g\downarrow} + |E_b|}{\hbar} + \frac{\hbar\left(|\mathbf{k}_{\mathrm{L}}|^2 + 2\mathbf{K}\cdot\mathbf{k}_{\mathrm{L}}\right)}{4m}. \tag{58}$$

Similarly, since in process (II) the atoms emit a photon, this this process can occur under the condition

$$E_0 - \hbar\omega_{\mathrm{L}} > E_{\min}^{(\mathrm{II})}, \tag{59}$$

where $E_{\min}^{(\mathrm{II})}$ is the minimum energy of the finial states of process (II), and can be expressed as

$$E_{\min}^{(\mathrm{II})} = E_{g\uparrow} + E_{g\downarrow} + \frac{\hbar^2|\mathbf{K}-\mathbf{k}_{\mathrm{L}}|^2}{4m}. \tag{60}$$

Using this result, we can re-express the energy condition (59) for process (II) as

$$\omega_{\mathrm{L}} < \omega_{\mathrm{II}}(\mathbf{K}) \equiv \frac{E_{e\uparrow} - E_{g\uparrow} - |E_b|}{\hbar} - \frac{\hbar\left(|\mathbf{k}_{\mathrm{L}}|^2 - 2\mathbf{K}\cdot\mathbf{k}_{\mathrm{L}}\right)}{4m}. \tag{61}$$

The above analysis yields that the laser-induced dissociation process can only occur under the condition (58) or (61). In particular, the dissociation process cannot occur in the frequency region $\omega_{\mathrm{II}} < \omega < \omega_{\mathrm{I}}$. Thus, the clock-transition spectrum includes two branches corresponding to process (I) and (II), respectively.

Our above analysis can be verified by the quantitative calculation for the dissociation rate based on the Fermi's golden rule. We consider two atoms with initial wave function

$$|\Psi(\mathbf{R},\mathbf{r},0)\rangle = \frac{1}{(2\pi)^{\frac{3}{2}}}\int d\mathbf{K}\phi(\mathbf{K})e^{i\mathbf{K}\cdot\mathbf{R}}|\phi_b(r)\rangle, \tag{62}$$

where $\mathbf{R}$ and $\mathbf{r}$ are the mass-center position and the relative position of these two atoms, respectively, $|\phi_b(r)\rangle$ is the two-atom bound sate wave function we obtained in the above subsection, and $\phi(\mathbf{K})$ is the wave function of the CoM motion in the momentum space. We further assume that the laser beam is applied from the time $t = 0$.

At time t the probability of the two atoms being in the bound state can be denoted as $P(t)$. The Fermi's golden rule yields that (Appendix B) when t is short we have [26]

$$P(t) \approx 1 - \Gamma t. \tag{63}$$

Here Γ is the dissociation rate. Furthermore, as shown in Appendix B for our system it can be proved that

$$\Gamma = \int d\mathbf{K}|\phi(\mathbf{K})|^2\gamma(\mathbf{K}), \tag{64}$$

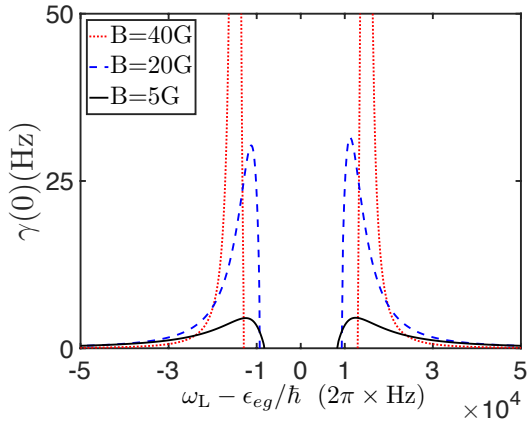

FIG. 6: The clock-transition spectrum for two ^{173}Yb atoms in bound state $|\phi_b(r)\rangle$ with $B = 5$G ($|E_b| = \hbar \times (2\pi)5176.05$Hz, black solid line), 20G ($|E_b| = \hbar \times (2\pi)2007.59$Hz, blue dashed line) and 40G ($|E_b| = \hbar \times (2\pi)22.63$Hz, red dotted line). In our calculation we take $m_I = -5/2$, $\Delta_m = 5$, $\Omega = (2\pi)10^3$Hz, $\epsilon_{eg} = \hbar \times (2\pi)5.19 \times 10^{14}$Hz [24, 25], $a_{gg} = 199.4a_0$, $a_{ee} = 306.2a_0$ [15], and $\mu_e - \mu_g = \hbar \times (2\pi)112$Hz/Gauss. The maximum value of $\gamma(\mathbf{0})$ for $B = 40$G is 772Hz. For a given magnetic field, the right and left branch of the spectrum corresponds to transition processes (I) and (II), respectively.

where $\gamma(\mathbf{K})$ is the dissociation rate corresponding to the mass-center momentum $\hbar\mathbf{K}$, and can be expressed as

$$\gamma(\mathbf{K}) = \gamma_{\mathrm{I}}(\mathbf{K}) + \gamma_{\mathrm{II}}(\mathbf{K}). \tag{65}$$

Here $\gamma_l(\mathbf{K})$ ($l = \mathrm{I}, \mathrm{II}$) is the dissociate rate for process (l), and is given by

$$\gamma_l(\mathbf{K}) = \frac{2\pi}{\hbar}\sum_{j=1,2}\int d\mathbf{k}\left|\int d\mathbf{r}\langle\Psi_j^l(\mathbf{k},\mathbf{r})|\Lambda(\mathbf{r})|\phi_b(r)\rangle\right|^2 \times\delta\left(\hbar\omega_l(\mathbf{K}) + \xi_l\frac{\hbar^2|\mathbf{k}|^2}{2m} - \hbar\omega_{\mathrm{L}}\right), \tag{66}$$

with $\xi_{\mathrm{I}} = 1$, $\xi_{\mathrm{II}} = -1$ and $\omega_{\mathrm{I,II}}(\mathbf{K})$ being defined in Eqs (58, 61). Here the operator $\Lambda(\mathbf{r})$ being defined as $\Lambda(\mathbf{r}) = \frac{\hbar\Omega}{2}(|e\rangle^{(1)}\langle g|e^{i\mathbf{k}_{\mathrm{L}}\cdot\mathbf{r}/2} + |e\rangle^{(2)}\langle g|e^{-i\mathbf{k}_{\mathrm{L}}\cdot\mathbf{r}/2} + h.c.$, where Ω is the Rabi frequency of the laser and $|e(g)\rangle^{(i)}$ ($i = 1, 2$) denotes the electronic orbital state of the i-th atom. In Eq. (66) $|\Psi_j^l(\mathbf{k},\mathbf{r})\rangle$ ($l = \mathrm{I}, \mathrm{II}$, $j = 1, 2$) is the finial state of process (l), i.e., the scattering state of two atoms with incident momentum $\mathbf{k}$ and two-atom electronic orbital state $|l\rangle$ and two-atom nuclear-spin state $|j\rangle$, which are defined as $|\mathrm{I}\rangle = |ee\rangle$, $|\mathrm{II}\rangle = |gg\rangle$, $|1\rangle = (|\uparrow\downarrow\rangle + |\downarrow\uparrow\rangle)/\sqrt{2}$ and $|2\rangle = (|\uparrow\downarrow\rangle - |\downarrow\uparrow\rangle)/\sqrt{2}$.

Furthermore, Eq. (64) implies that if the mass-center momentum is mainly distributed in a small region around a central momentum $\mathbf{K}_0$, we have $\Gamma \approx \gamma(\mathbf{K}_0)$. In the following we consider the simple case with $\mathbf{K}_0 = \mathbf{0}$. We further calculate $\gamma(\mathbf{0})$ for ^{173}Yb atoms for the cases with different magnetic field. Our calculation is based on the binding energy E_b and the closed-channel population Z

derived with the MQDT in Sec. III. A. On the other hand, since in our system both E_b and the energy gap δ between the open and closed channels are much smaller than the van der Waals energy, in the bound state $|\phi_b(r)\rangle$ the two-atom relative position r is mainly distributed in the region $r \gtrsim \beta_6$. Thus, in our calculation we ignore the contribution from the two-atom relative function $|\phi_b(r)\rangle$ in the region $r \lesssim \beta_6$ and use the approximated bound-state wave function

$$|\phi_b(r)\rangle = \sqrt{1-Z}\frac{e^{-r/r_o}}{\sqrt{2\pi r_o r}}|o\rangle + \sqrt{Z}\frac{e^{-r/r_c}}{\sqrt{2\pi r_c r}}|c\rangle, \quad (67)$$

and the approximated scattering-state wave functions

$$|\Psi_j^l(\mathbf{k},\mathbf{r})\rangle = \frac{1}{(2\pi)^{\frac{3}{2}}}\left[e^{i\mathbf{k}\cdot\mathbf{r}} + \frac{-1}{ik+\frac{1}{a_l}}e^{ikr}\right]|l\rangle|j\rangle;$$
$$\text{for } l = \text{I, II and } j = 1,2. \quad (68)$$

Here $r_o = \hbar/\sqrt{2m|E_b|}$, $r_c = \hbar/\sqrt{2m(|E_b|+\delta)}$, $a_{\rm I} = a_{ee}$, and $a_{\rm II} = a_{gg}$, with a_{ee} (a_{gg}) being the scattering length of two atoms who are both in e-state (g-state).

In Fig.(6) we show $\gamma(\mathbf{0})$ as a function of $\omega_{\rm L}$ for ^{173}Yb atoms with various magnetic field. It is clear that for each magnetic field the clock-transition spectrum has two branches, corresponding to process (I) (right branch with $\omega_{\rm L} > \omega_{\rm I}$) and process (II) (left branch with $\omega_{\rm L} < \omega_{\rm II}$), as we have analyzed before. Furthermore, it is also shown that when the magnetic field is close to the OFR point B_0, the spectrum becomes more sharp. This result may be explained as follows. When the system is close to the OFR point, the wave packet of the bound state becomes very wide in the real space, and thus very narrow in the momentum space. Therefore, in this case the bound state has significant overlap (the Frank-Condon factor) only with the the scattering states $|\Psi_j^l(\mathbf{k},\mathbf{r})\rangle$ with incident momentum and scattering energy being in a small region, and thus the transition spectrum becomes narrow.

Our above results, together with Eqs. (58, 61), show that both the position and the shape of the clock-transition spectrum are related to the binding energy E_b and the wave function of the two-body bound state $|\phi_b(r)\rangle$. Thus, in the experiments one can detect the properties of $|\phi_b(r)\rangle$ via the clock-transition spectrum.

IV. SUMMARY

In this paper we solve the two-body problem of two alkali-earth (like) atoms with OFR with the approach of MQDT, in which the effect induced by the van der Waals interaction potential can be analytically included. We derive the analytical expression of the scattering length (Eq. (42)) and the effective range (Eq. (43)), as well as the algebraic equation (52) for the binding energy of the two-body bound state. We further investigate the clock-transition spectrum for our system, which can be used for the experimental detection of the bound state. Since the MQDT approach is quantitatively applicable for the system where the all the characteristic energies are much smaller than the van der Waals energy, e.g., the ^{173}Yb atoms near the OFR point, our results are helpful for both theoretical and experimental research for these systems.

Acknowledgments

We thank Bo Gao and Hui Zhai for helpful discussions. This work has been supported by the Natural Science Foundation of China under Grant No. 11434011, and by NKBRSF of China under Grant No. 2012CB922104, the Fundamental Research Funds for the Central Universities, and the Research Funds of Renmin University of China under Grant No.16XNLQ03.

Appendix A: The ϵ- and δ-dependence of K_{ij}^0

In this appendix we show that the parameters K_{ij}^0 in Sec. II. B are independent of ϵ and δ. This fact can be understood with the following arguments.

First, the conditions (7, 8) imply that there is a spatial region in which both of the two conditions $r > b$ and $\hbar^2\beta_6^4/(mr^6) >> \hbar^2/(m\beta_6^2)$ are satisfied. Here we denote this region as $\mathcal{R}$.

Second, similar as in Sec. II. A, due to the conditions (7, 8) and the fact that both ϵ and δ are much smaller than $\hbar^2/(m\beta_6^2)$, in both region $\mathcal{R}$ and the region of $r < b$, these two energies can be neglected from the Schrödinger equation (10). Thus, we know that Eq. (10) and the condition (11) have two special solutions which are independent of ϵ and δ in the region of $\mathcal{R}$ and the region of $r < b$. We denote these two solutions as $|\Phi_1(r)\rangle$ and $|\Phi_2(r)\rangle$.

Third, since both $|\psi_{\epsilon,\delta}^{(\alpha,\beta)}(r)\rangle$ introduced in Sec. II. B and $|\Phi_{1,2}(r)\rangle$ are special solutions of Eqs. (10, 11), $|\psi_{\epsilon,\delta}^{(\alpha,\beta)}(r)\rangle$ can be expressed as linear superpositions of $|\Phi_{1,2}(r)\rangle$. Namely, we have

$$|\psi_{\epsilon,\delta}^{(l)}(r)\rangle = \sum_{j=1,2} A_j^{(l)}|\Phi_j(r)\rangle. \quad (A1)$$

Here the coefficients $A_j^{(l)}$ ($l = \alpha,\beta$, $j = 1,2$) are determined by the following two conditions given by Eqs. (25, 26): (a) For $r \in \mathcal{R}$, if one expand $r\langle c|\psi_{\epsilon,\delta}^{(\alpha)}(r)\rangle$ as a superposition of the functions $f_{\epsilon-\delta}^0(r)$ and $g_{\epsilon-\delta}^0(r)$, then the coefficient for $f_{\epsilon-\delta}^0(r)$ is zero. (b) For $r \in \mathcal{R}$, if one expand $r\langle o|\psi_{\epsilon,\delta}^{(\alpha)}(r)\rangle$ as a superposition of the functions $f_\epsilon^0(r)$ and $g_\epsilon^0(r)$, then the coefficient for $g_\epsilon^0(r)$ is zero. Since these two conditions are independent of K_{ij}^0 the value of $A_j^{(l)}$ ($l = \alpha,\beta$, $j = 1,2$) is also independent of K_{ij}^0. Furthermore, since in the region $\mathcal{R}$ both $|\Phi_{1,2}(r)\rangle$ and the functions $f_\epsilon^0(r)$, $g_\epsilon^0(r)$, $f_{\epsilon-\delta}^0(r)$ and $g_{\epsilon-\delta}^0(r)$ are

independent of ϵ and δ [17], it is clear that the coefficients $A_j^{(l)}$ determined by the above two conditions are also (ϵ,δ)-independent. Therefore, the right-hand side of Eq. (A1) is independent of ϵ and δ for $r\in\mathcal{R}$. Using this result and Eqs. (25, 26), we immediately know that K_{ij}^0 in Sec. II. B are independent of ϵ and δ.

Appendix B: Calculation of dissociation rate

In this appendix we calculate the dissociation rate of two-atom bound state and prove Eqs. (64, 65, 66). In the Schrödinger picture, the Hamiltonian for our problem is given by

$$H=\frac{-\hbar^2\nabla_{\mathbf{R}}^2}{4m}+H_I+H_{\rm rel}+H_{\rm L} \tag{B1}$$

where $\mathbf{R}$ is the two-atom center of mass (CoM) position. Here H_I describeds the one-body internal-state energy and is given by

$$H_I=\sum_{j=1,2}\sum_{l=e,g}\sum_{s=\uparrow,\downarrow}E_{ls}|l,s\rangle^{(j)}\langle l,s|, \tag{B2}$$

with $|l,s\rangle^{(j)}$ $(j=1,2;\ l=e,g;\ s=\uparrow,\downarrow)$ being the internal state of the s-th atom and E_{lj} being the corresponding one-body energy, which is defined in Sec. III.B. In Eq. (B1) $H_{\rm rel}$ and $H_{\rm L}$ are the Hamiltonian for the two-atom relative motion and laser-atom coupling, respectively, and can be expressed as

$$H_{\rm rel} = \frac{-\nabla_{\mathbf{r}}^2}{m}+U_T(\mathbf{r}); \tag{B3}$$

$$H_{\rm L} = \frac{\hbar\Omega}{2}\sum_{j=1,2}|e\rangle^{(j)}\langle g|e^{i(\mathbf{k}_{\rm L}\cdot\mathbf{r}_j-\omega_{\rm L}t)}+h.c.. \tag{B4}$$

Here $\mathbf{r}$ is the two-atom relative position, $|e(g)\rangle^{(j)}$ $(j=1,2)$ is the electronic-orbital state of the j-th atom, $U_T(\mathbf{r})$ is the total interaction potential, Ω is the Rabi frequency of the clock laser beam, and $\mathbf{k}_{\rm L}$ and $\omega_{\rm L}$ being the wave vector and angular frequency of this laser beam, respectively. In Eq. (B4) $\mathbf{r}_j$ $(j=1,2)$ is the position of the j-th atom, and can be expressed as

$$\mathbf{r}_1 = \mathbf{R}+\frac{\mathbf{r}}{2}; \tag{B5}$$

$$\mathbf{r}_2 = \mathbf{R}-\frac{\mathbf{r}}{2}. \tag{B6}$$

As shown in Eq. (62) of Sec. III.B, we assume that at $t=0$ the two-atom initial wave function is

$$|\Psi(\mathbf{R},\mathbf{r},t=0)\rangle=\frac{1}{(2\pi)^{\frac{3}{2}}}\int d\mathbf{K}\phi(\mathbf{K})e^{i\mathbf{K}\cdot\mathbf{R}}|\phi_b(r)\rangle, \tag{B7}$$

where $|\phi_b(r)\rangle$ is the wave function of the two-atom bound state. We further assume that the laser beam is applied from $t=0$. Thus, for $t\geq 0$ the evolution of the two atoms is governed by the total Hamiltonian H. At time t the two-atom wave function can be denoted as $|\Psi(\mathbf{R},\mathbf{r},t)\rangle$, and the probability of these two atoms being at the bound state $|\phi_b(r)\rangle$ can be expressed as

$$P(t)=\int d\mathbf{R}\int d\mathbf{r}\,|\langle\phi_b(r)|\Psi(\mathbf{R},\mathbf{r},t)\rangle|^2. \tag{B8}$$

To calculate $P(t)$ with the Fermi's golden rule, we introduce a unitary transformation

$$\mathcal{U}=e^{-i\mathbf{k}_L\cdot\mathbf{R}\Sigma_e} \tag{B9}$$

where

$$\Sigma_e=|ee\rangle\langle ee|-|gg\rangle\langle gg|. \tag{B10}$$

We further define the wave function $|\Phi(\mathbf{R},\mathbf{r},t)\rangle$ as

$$|\Phi(\mathbf{R},\mathbf{r},t)\rangle=\mathcal{U}|\Psi(\mathbf{R},\mathbf{r},t)\rangle, \tag{B11}$$

i.e., $|\Phi(\mathbf{R},\mathbf{r},t)\rangle$ is the two-atom state in the rotated frame induced by $\mathcal{U}$. It is easy to prove that we have

$$|\Phi(\mathbf{R},\mathbf{r},t=0)\rangle = |\Psi(\mathbf{R},\mathbf{r},t=0)\rangle; \tag{B12}$$

$$P(t) = \int d\mathbf{R}\int d\mathbf{r}\,|\langle\phi_b(r)|\Phi(\mathbf{R},\mathbf{r},t)\rangle|^2. \tag{B13}$$

Furthermore, we can also prove that $|\Phi(\mathbf{R},\mathbf{r},t)\rangle$ satisfies the Schrödinger equation

$$i\hbar\frac{d}{dt}|\Phi(\mathbf{R},\mathbf{r},t)\rangle=H_{\rm rot}|\Phi(\mathbf{R},\mathbf{r},t)\rangle \tag{B14}$$

with $H_{\rm rot}$ being the Hamiltonian in the rotated frame and can be expressed as

$$H_{\rm rot} = \frac{(-i\hbar\nabla_{\mathbf{R}}+\hbar\mathbf{k}_{\rm L}\Sigma_e)^2}{4m}+H_I+H_{\rm rel}+h_{\rm L}, \tag{B15}$$

with

$$h_{\rm L} = \frac{\hbar\Omega}{2}e^{-i\omega_{\rm L}t}\left(|e\rangle^{(1)}\langle g|e^{i\mathbf{k}_{\rm L}\cdot\mathbf{r}/2}+|e\rangle^{(2)}\langle g|e^{-i\mathbf{k}_{\rm L}\cdot\mathbf{r}/2}\right) +h.c.. \tag{B16}$$

Eq. (B15) shows that in the rotated frame the momentum of the CoM is conserved. Using this fact and Eqs. (B12) and (B7), we can simplify the calculation of the probability $P(t)$ in Eq. (B13) and obtain

$$P(t)=\int d\mathbf{K}|\phi(\mathbf{K})|^2p(\mathbf{K}) \tag{B17}$$

where $p(\mathbf{K})$ is given by

$$p(\mathbf{K})=\int d\mathbf{r}\,|\langle\phi_{\mathbf{K}}(\mathbf{r},t)|\phi_b(r)\rangle|^2. \tag{B18}$$

Here the wave function $|\phi_{\mathbf{K}}(\mathbf{r},t)\rangle$ satisfies the equation

$$i\frac{d}{dt}|\phi_{\mathbf{K}}(\mathbf{r},t)\rangle = h(\mathbf{K})|\phi_{\mathbf{K}}(\mathbf{r},t)\rangle \tag{B19}$$

with

$$h(\mathbf{K}) = \frac{-\hbar^2\nabla_{\mathrm{r}}^2}{m} + H_I + U(\mathbf{r}) + \frac{(\hbar\mathbf{K}+\hbar\mathbf{k}_{\mathrm{L}}\Sigma_e)^2}{4m} + h_{\mathrm{L}}. \tag{B20}$$

$$\equiv h_0(\mathbf{K}) + h_{\mathrm{L}}, \tag{B21}$$

as well as the initial condition

$$|\phi_{\mathbf{K}}(\mathbf{r},t=0)\rangle = |\phi_b(r)\rangle. \tag{B22}$$

Eqs. (B18-B22) show that to calculate $p(\mathbf{K})$ we need to solve a quantum evolution problem governed by the Hamiltonian $h(\mathbf{K})$. This problem is defined in the Hilbert space $\mathcal{H}_r \otimes \mathcal{H}_I$, with $\mathcal{H}_r$ and $\mathcal{H}_I$ being the space for two-atom spatial relative motion and two-atom internal state, respectively, and the CoM momentum $\hbar\mathbf{K}$ just behaves as a classical parameter (c-number). In this problem, the term h_{L} induces the transitions from the isolated state $|\phi_b(r)\rangle$, which is a discrete eigen-state of $h_0(\mathbf{K})$, to other continuous eigen-states of $h_0(\mathbf{K})$, i.e., the scattering states of two atoms in either the electronic-orbital state $|ee\rangle$ or $|gg\rangle$. Thus, we can calculate $p(\mathbf{K})$ using the Fermi's golden rule and obtain that when the time t is small enough we have [26]

$$p(\mathbf{K}) = 1 - \gamma(\mathbf{K})t \tag{B23}$$

where $\gamma(\mathbf{K})$ is given by Eqs. (65, 66) in Sec. III. B. Furthermore, substituting Eq. (B23) into Eq. (B17) and using Eq. (63) in Sec. III. B, we can obtain Eq. (64) in Sec. III. B.

[1] H. Feshbach, Ann. Phys. **5**, 357 (1958).
[2] C. Chin, R. Grimm, P. Julienne and E. Tiesinga, Rev. Mod. Phys. **82**, 1225 (2010).
[3] R. Zhang, Y. Cheng, H. Zhai, and P. Zhang, Phys. Rev. Lett. **115**, 135301 (2015).
[4] G. Pagano, M. Mancini, G. Cappellini, L. Livi, C. Sias, J. Catani, M. Inguscio, L. Fallani, Phys. Rev. Lett. **115**, 265301 (2015).
[5] M. Höfer, L. Riegger, F. Scazza, C. Hofrichter, D.R. Fernandes, M. M. Parish, J. Levinsen, I. Bloch, S. Fölling, Phys. Rev. Lett. **115**, 265302 (2015)
[6] R. Zhang, D. Zhang, Y. Cheng, W. Chen, P. Zhang, and H. Zhai, Phys. Rev. A **93**, 043601 (2016).
[7] J. Xu, R. Zhang, Y. Cheng, P. Zhang, R. Qi and H. Zhai, arXiv: 1602.06513.
[8] L. Isaev, J. Schachenmayer, and A. M. Rey, arXiv:1603.01946.
[9] S. Capponia, P. Lecheminantb, and K. Totsukac, Ann. Phys. **367**, 50 (2016).
[10] V. Bois, P. Fromholz, P. Lecheminant, Phys. Rev. B **93**, 134415 (2016).
[11] M. Iskin, arXiv:1605.00470.
[12] L. He, J. Wang, S. Peng, X. Liu and Hui Hu, arXiv: 1606.00188.
[13] R. Qi, arXiv:1606.03299.
[14] Y. Zhang, S. Ding, S. Zhang, arXiv: 1606.07168.
[15] X. Zhang, M. Bishof, S. L. Bromley, C. V. Kraus, M. S. Safronova, P. Zoller, A. M. Rey, J. Ye., Science, **345**, 1467 (2014).
[16] Y. Cheng, R. Zhang, and P. Zhang, Phys. Rev. A **93**, 042708 (2016).
[17] B. Gao, Phys. Rev. A **58**, 1728 (1998). The functions $f^0_{\epsilon,l=0}(r)$ and $g^0_{\epsilon,l=0}(r)$ in this reference are denoted as $f^0_{\epsilon}(r)$ and $g^0_{\epsilon}(r)$ in this paper, respectively.
[18] B. Gao, Phys. Rev. A **58**, 4222 (1998).
[19] B. Gao, Phys. Rev. A **62**, 050702(R) (2000).
[20] B. Gao, Phys. Rev. A **64**, 010701(R) (2001).
[21] B. Gao, E. Tiesinga, C. J. Williams, and P. S. Julienne Phys. Rev. A **72**, 042719 (2005).
[22] B. Gao, Phys. Rev. A **80**, 012702 (2009).
[23] B. Gao, Phys. Rev. A **84**, 022706 (2011).
[24] G. Cappellini, M. Mancini, G. Pagano, P. Lombardi, L. Livi, M. Siciliani de Cumis, P. Cancio, M. Pizzocaro, D. Calonico, F. Levi, C. Sias, J. Catani, M. Inguscio, and L. Fallani, Phys. Rev. Lett. **113**, 120402 (2014).
[25] F. Scazza, C. Hofrichter, M. Höfer, P. C. De Groot, I. Bloch, and S. Fölling, Nature Phys. **10**, 779 (2014).
[26] Precisely speaking, the Fermi's golden rule is applicable when both of the following two conditions are satisfied: (a) t is short enough so that the atom-laser coupling can be considered as a lowest-order perturbation. (b) t is much longer than the correlation time of the laser-induced coupling between the bound state and the scattering states.